The accuracy of the DDA (Discrete Dipole Approximation) method in determining the optical properties of black carbon fractal-like aggregates

Krzysztof Skorupski[a]

[a]Wroclaw University of Technology, Chair of Electronics and Photonics Metrology, Boleslawa Prusa 53/55, 50-317 Wroclaw, Poland

ABSTRACT

Black carbon (BC) particles are a product of incomplete combustion of carbon-based fuels. One of the possibilities of studying the optical properties of BC structures is to use the DDA (Discrete Dipole Approximation) method. The main goal of this work was to investigate its accuracy and to approximate the most reliable simulation parameters. For the light scattering simulations the ADDA code was used and for the reference program the superposition T-Matrix code by Mackowski was selected. The study was divided into three parts. First, DDA simulations for a single particle (sphere) were performed. The results proved that the meshing algorithm can significantly affect the particle shape, and therefore, the extinction diagrams. The volume correction procedure is recommended for sparse or asymmetrical meshes. In the next step large fractal-like aggregates were investigated. When sparse meshes are used, the impact of the volume correction procedure cannot be easily predicted. In some cases it can even lead to more erroneous results. Finally, the optical properties of fractal-like aggregates composed of spheres in point contact were compared to much more realistic structures made up of connected, non-spherical primary particles.

Keywords: discrete dipole approximation, light scattering, black carbon, soot

1. INTRODUCTION

Small particles tend to connect to each other and create large structures called aggregates. Their complex shape can be described by the following fractal equation:[1]

$$N_p = k_f \left(\frac{R_g}{r_p} \right)^{D_f}, \tag{1}$$

where N_p is the number of primary particles with the radius r_p. The fractal prefactor (a proportionality constant) is denoted as k_f. The compactness of the structure is characterized by the fractal dimension which varies from $D_f \approx 1$ (e.g. primary particles form a straight line) to $D_f \approx 3$ (e.g. primary particles form a compact ball). The last parameter, namely the radius of gyration R_g, can be calculated with the following equation:[2]

$$R_g^2 = \frac{1}{N_p} \sum_{i=1}^{N_p} (\vec{r}_i - \vec{r}_c)^2, \tag{2}$$

where $\vec{r}$ is the position of the i-th primary particle and $\vec{r}_c$ is the mass centre of the aggregate. This is a reliable approximation providing that monodisperse primary particles are positioned in point contact (they are connected but do not intersect). Note, that every morphological parameter has an impact on the optical properties of investigated geometries.[3] Fractal-like aggregate models used in this study were generated using the tunable CC (Cluster-Cluster) algorithm proposed by Filippov et al.[4,5] It guarantees that the fractal equation Eq. (1) is true for every step of the aggregation process. More information about the aggregation phenomenon can be found elsewhere, e.g. in the work by Meakin.[6]

E-mail: krzysztof.skorupski@pwr.edu.pl

Nonlinear Optics and Applications IX, edited by Mario Bertolotti, Joseph W. Haus, Alexei M. Zheltikov,
Proc. of SPIE Vol. 9503, 95030U · © 2015 SPIE · CCC code: 0277-786X/15/$18 · doi: 10.1117/12.2178646

This research was focused on BC (black carbon) aggregates. Due to their absorption properties it is assumed that they have impact on the global warming effect, and therefore, are a matter of concern for many climate scientists.[7,8] BC aggregates may consist of a few or even a few hundred primary particles with the radius $r_p \approx 15nm$. The fractal parameters are $D_f \approx 2.2$ and $k_f \approx 0.8$ respectively.[9] Note, that these values are rough approximations and may vary across publications.[10,11] The complex refractive index m was adapted from the paper by Chang and Charalampopoulos.[12] It is valid for particles generated in a propane-oxygen flame with the fuel equivalence ratio $\phi = 1.8$ and HAB (Height Above Burner) 10 mm. Additionally, it is in agreement with the criterion proposed by Bond et al.[13] Similarly to the morphological parameters, m is not considered universal and different values have been published.[14,15] The morphological parameters of fractal-like aggregates can be approximated using different techniques[16–28] which are based on different assumptions, and therefore, might lead to slightly different results.

The light scattering phenomenon can be modelled using different techniques.[29] In this work the DDA (Discrete Dipole Approximation) method was used.[30–33] It gives accurate results providing that the scatterer is divided into a sufficient number of volume elements (dipoles). The generated mesh must resemble the original geometry, and for this reason, it is recommended to put at least 10 volume elements (dipoles) along its smallest dimension.[34] Additionally, simulations in which materials are characterized by large values of the imaginary part of the complex refractive index m are much more time consuming and larger computational resources are required.[35] Although many DDA algorithms are available, only one of them, namely ADDA, was used.[34] It is widely recognized by the light scattering community and its frequent updates guarantee that results are reliable. Note, that light scattering codes are not limited to fractal-like aggregates and can be used with very different geometries, including e.g. erythrocytes and fibres.[36–41]

The incident wavelength varied from $\lambda = 300nm$ to $\lambda = 900nm$ with the step $\Delta\lambda = 20nm$. The polarizability expression was IGT and other ADDA parameters were set to their default values. A more detailed study about the impact of different parameters on DDA simulations for BC aggregates can be found elsewhere.[42] This paper is an extension of the work by Skorupski and covers a different set of topics which might help to approximate and diminish the simulation error.[42]

2. SIMULATION RESULTS

In the first part of the study a single, spherical BC particle was investigated. It was decomposed into different meshes of volume elements (dipoles) required for DDA simulations, as presented in Fig. 1 and described in Tab. 1 in more detail. Because the distance between mesh elements d was constant, the total volume of the scatterer V was slightly altered, i.e. $V \neq V_{ref}$ where V_{ref} is the volume of a primary particle with the radius $r_p = 15nm$. As the reference scattering code the superposition T-Matrix algorithm by Mackowski was used.[43] In this paper, the averaged relative extinction error δC_{ext} is the arithmetic mean of all absolute relative errors $|\delta C(\lambda)_{ext}|$.

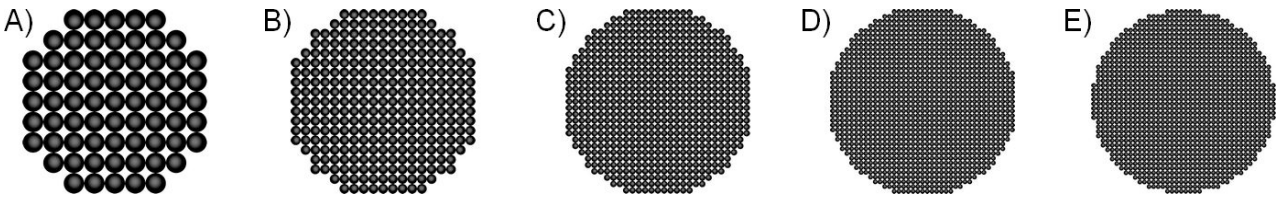

Figure 1. Different meshes of volume elements (dipoles) of a single BC particle required for DDA simulations. More information about each geometry can be found in Tab. 1.

Relative extinction errors $\delta C(\lambda)_{ext}$, which are presented in Fig. 2, cover two different simulation techniques. In one of them the volume correction procedure was used, i.e. the value of d was modified to fit the real volume of the investigated BC particle, what resulted in $V = V_{ref}$ (δV was negligible). The results show that the absolute value of $\delta C(\lambda)_{ext}$ decreases along with the number of volume elements (dipoles). When the volume correction procedure is used, diagrams are more smooth and predictable. However, in some cases they can be slightly more erroneous. The most significant improvement was observed for the most sparse mesh, namely M0.

Table 1. The description of the symmetrical DDA meshes presented in Fig. 1. The number of volume elements (dipoles) is denoted as N_d and the distance between them is d.

	M0	M1	M2	M3	M4
N_d	485	4139	13997	33371	65117
d $[nm]$	3.00	1.50	1.00	0.75	0.60

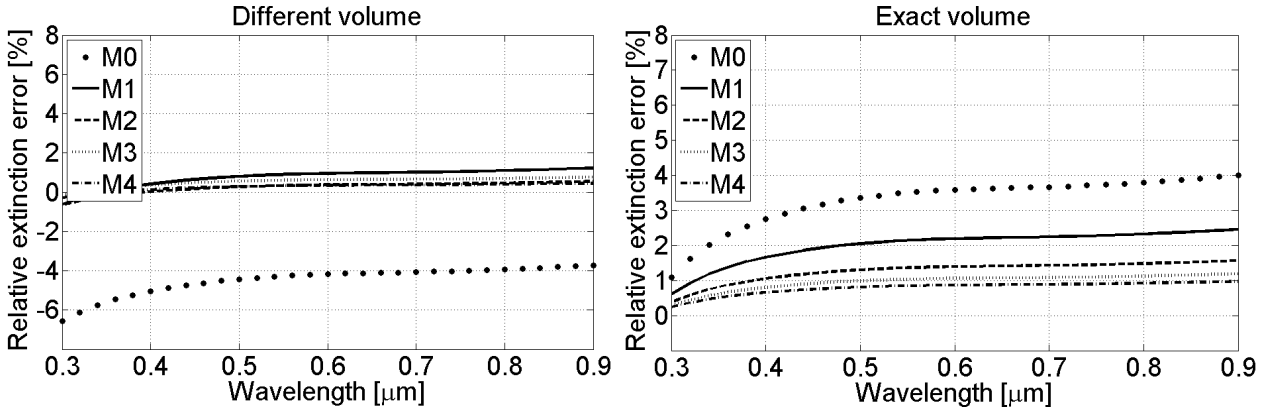

Figure 2. The relative extinction error $\delta C(\lambda)_{ext}$ for different meshes of volume elements (dipoles). Two simulation techniques are compared: without (right) and with (left) the volume correction procedure.

In the previous study the centre of the BC particle was positioned in the middle of the coordinate system, and therefore, every generated mesh was symmetrical. For the following simulations, the BC particle was translated by $t = l \cdot d$ along all three axes (X, Y and Z). After this procedure the symmetry was broken and many different meshes of volume elements (dipoles) were generated, as presented in Fig. 3. This is a more realistic approach, especially when large fractal-like aggregates are investigated and every BC particle is characterized by a slightly different mesh. Relative extinction errors for M0 are presented in Fig. 4. They prove that different meshes lead to very different results. However, when the volume correction procedure is used, resulting curves are much more similar to each other. The averaged relative extinction error δC_{ext} and the relative volume error δV can be found in Tab. 3.

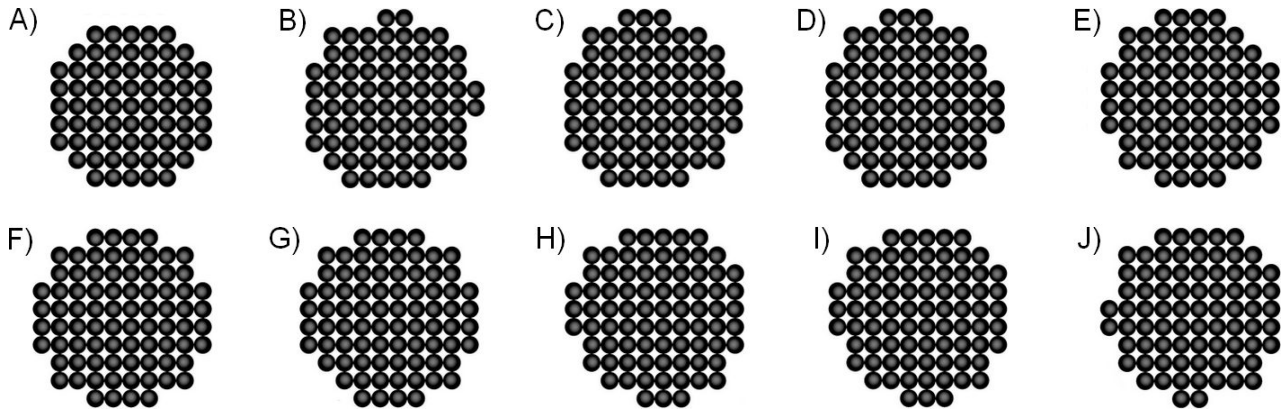

Figure 3. A single BC particle decomposed into different meshes of volume elements (dipoles). Each geometry is a result of a translation of the geometric centre of the investigated BC particle. The translation length varies from $l = 0.0$ to $l = 0.9$ with the step $\Delta l = 0.1$. The distance between volume elements (dipoles) is $d = 3nm$ in every case.

Table 2. The description of the meshes presented in Fig. 3. The number of volume elements (dipoles) is denoted as N_d. The relative volume error is δV. The distance between mesh elements is $d = 3nm$.

	A	B	C	-	D	E	F	G	H	-	I	J
l	0.00	0.10	0.20	0.25	0.30	0.40	0.50	0.60	0.70	0.75	0.80	0.90
N_d	485	515	516	528	522	522	552	522	522	528	516	515
δV [%]	-7.37	-1.64	-1.45	0.84	-0.31	-0.31	5.42	-0.31	-0.31	0.84	-1.45	-1.64

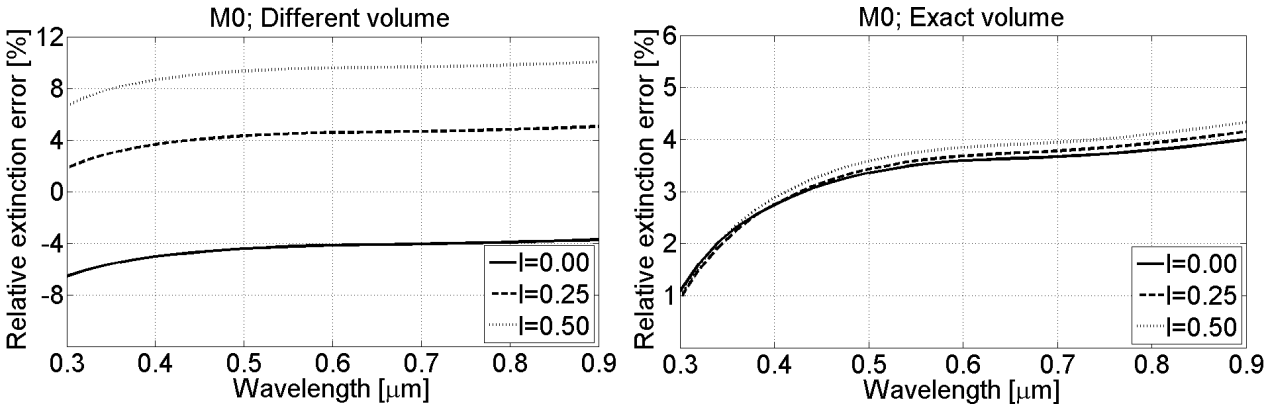

Figure 4. The relative extinction error $\delta C(\lambda)_{ext}$ for the most sparse mesh used in this study, namely M0 ($d = 3nm$), and three different translations: $l = 0.00$, $l = 0.25$ and $l = 0.50$.

Table 3. The averaged relative extinction error δC_{ext} and the relative volume error δV for geometries used in this study.

	Different volume, $V \neq V_{ref}$					Exact volume, $V = V_{ref}$				
	M0	M1	M2	M3	M4	M0	M1	M2	M3	M4
Translation	δV [%]					δV [%]				
$l = 0.00$	-7.37	-1.19	-0.99	-0.42	-0.51	-	-	-	-	-
$l = 0.25$	0.84	0.12	0.01	0.01	0.07	-	-	-	-	-
$l = 0.50$	5.42	0.84	1.35	0.12	0.46	-	-	-	-	-
Translation	δC_{ext} [%]					δC_{ext} [%]				
$l = 0.00$	4.46	0.84	0.36	0.55	0.31	3.30	2.01	1.28	0.97	0.80
$l = 0.25$	4.25	2.04	1.31	0.99	0.87	3.36	1.91	1.30	0.98	0.80
$l = 0.50$	9.24	2.70	2.68	1.13	1.28	3.51	1.82	1.29	1.00	0.81

Additionally, the orientational averaging procedure[2] was used to check whether the rotation of a non-perfect mesh of volume elements (dipoles) influences DDA results. The averaging was performed using the Romberg integration technique in the adaptive regime. The estimated integration error was 0.001 and the maximum number of orientations was 256. As expected, the results were slightly different. However, the difference between DDA curves was lower than 0.1% in every case, and therefore, it was considered negligible. Averaged results were compared to those presented in Tab. 3 (30 different geometries were investigated).

In the next part of this study four different fractal-like BC aggregates were generated (see Fig. 5). They consisted of $N_p = 25$, $N_p = 50$, $N_p = 75$ and $N_p = 100$ spherical particles positioned in point contact. Simulations for M0, i.e. when $d = 3nm$, were performed for fixed orientations and the corresponding extinction diagrams are presented in Fig. 6. Fig. 7 in Fig. 8 present the relative extinction error $\delta C(\lambda)_{ext}$. The diagrams show two orthogonal polarization states, namely A (plane ZX) and B (plane ZY). The impact of the volume correction procedure turned out not to be as significant as before, i.e. when a single particle was investigated. The absolute volume error $|\delta V|$ was already low and did not exceed the value of 0.24% in any case. The results for M1, i.e.

when $d = 1.5nm$, are presented in Fig. 9 and in Fig. 10. For these meshes the initial absolute volume error $|\delta V|$ was always lower than 0.13%. In this case, when the volume correction procedure was used, resulting curves were more similar to each other, regardless of the number of primary particles N_p. Note, that the volume correction procedure might shrink or enlarge the investigated mesh, and therefore, the centres of primary particles can be slightly moved. More information about the extinction error when different DDA parameters are used can be found elsewhere.[42]

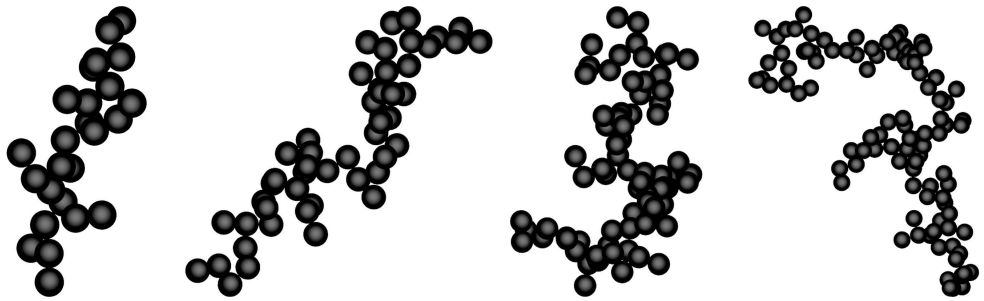

Figure 5. Fractal-like aggregates composed of $N_p = 25$, $N_p = 50$, $N_p = 75$ and $N_p = 100$ primary particles. The geometries were generated using the tunable CC (Cluster-Cluster) algorithm by Filippov.[4]

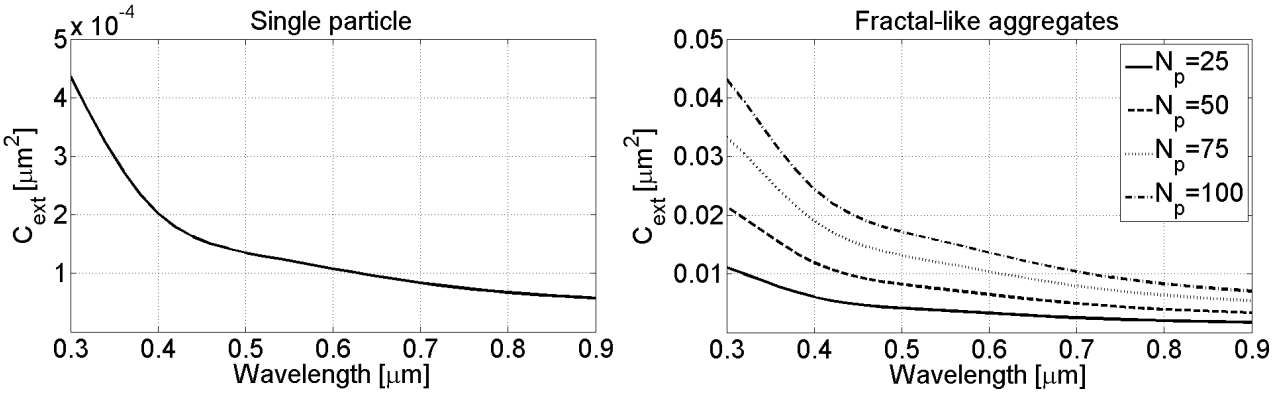

Figure 6. The extinction diagrams for BC structures used in this study. Only one polarization state, i.e. A (plane ZX), is presented. The results were calculated using the T-Matrix code.

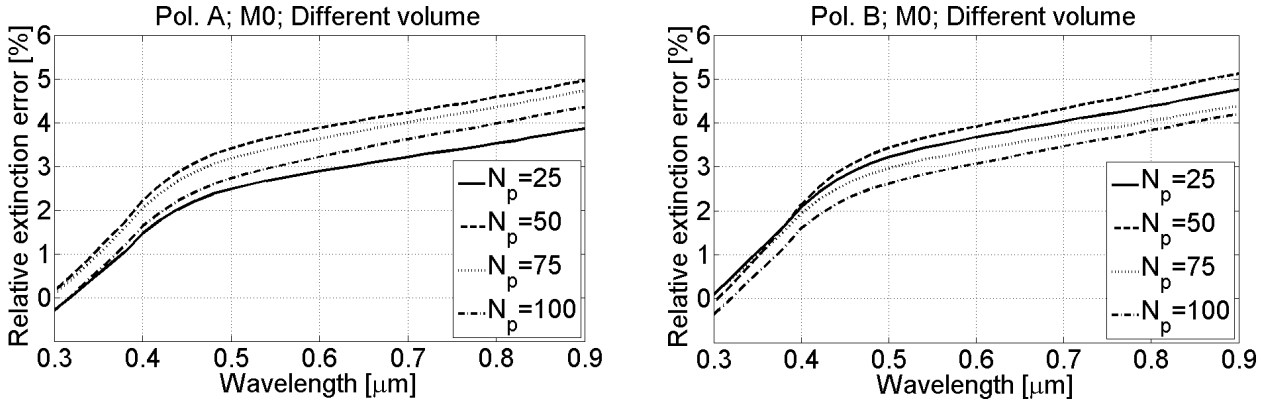

Figure 7. The relative extinction error $\delta C(\lambda)_{ext}$ for fractal-like aggregates. The volume correction procedure was not used and the light scattering results were not averaged. The distance between volume elements (dipoles) was $d = 3nm$.

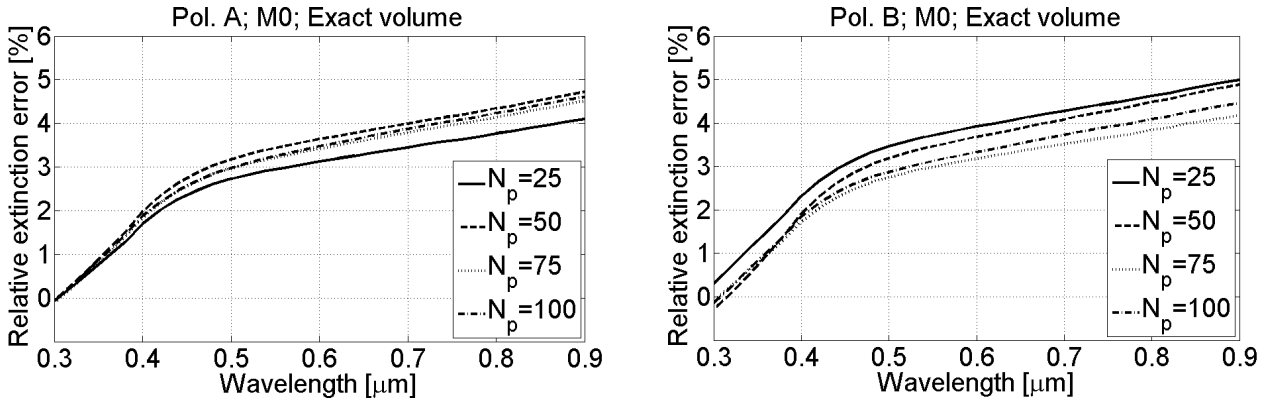

Figure 8. The relative extinction error $\delta C(\lambda)_{ext}$ for fractal-like aggregates. The volume correction procedure was used. The results were not averaged and the distance between volume elements (dipoles) was $d = 3nm$.

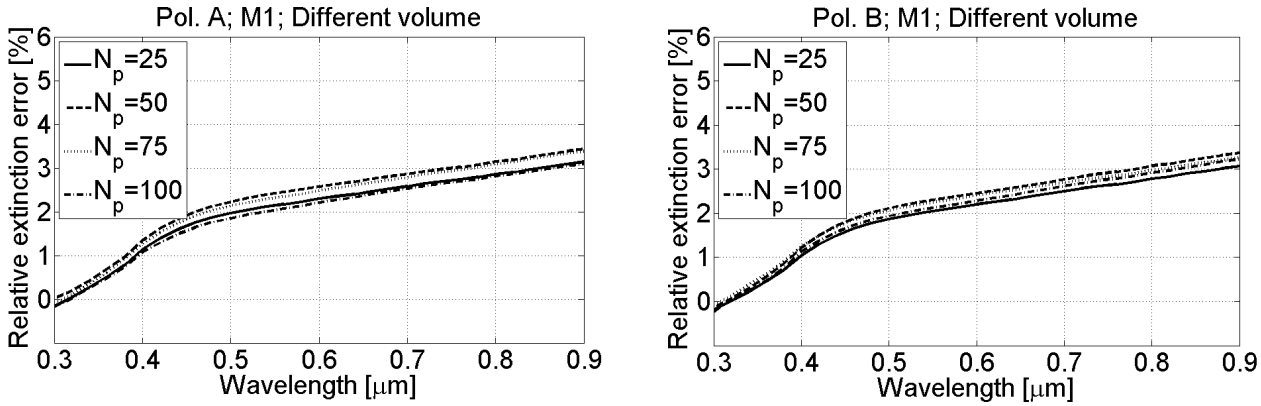

Figure 9. The relative extinction error $\delta C(\lambda)_{ext}$ for fractal-like aggregates. The volume correction procedure was not used and the light scattering results were not averaged. The distance between volume elements (dipoles) was $d = 1.5nm$.

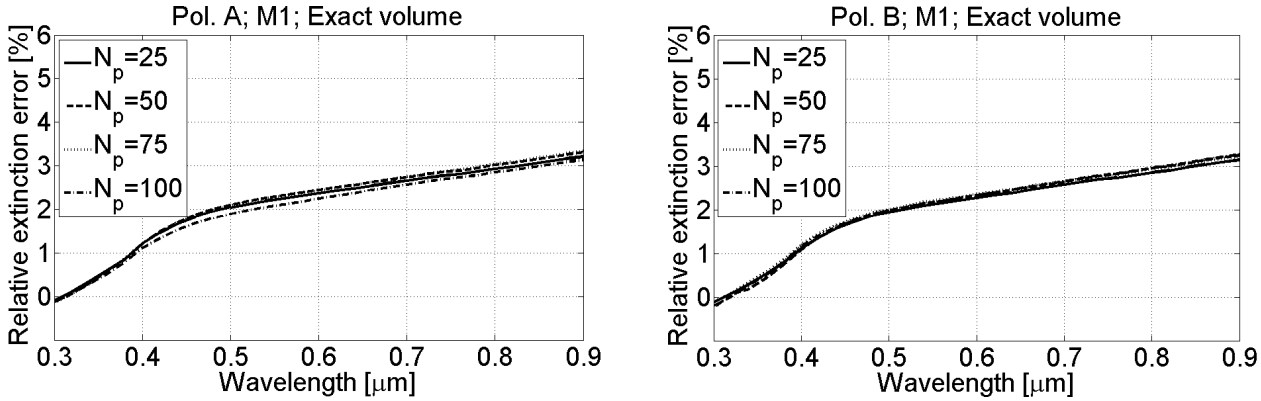

Figure 10. The relative extinction error $\delta C(\lambda)_{ext}$ for fractal-like aggregates. The volume correction procedure was used. The results were not averaged and the distance between volume elements (dipoles) was $d = 1.5nm$.

Next, primary particles were replaced with ellipsoids characterized by the following morphological parameters: $r_{avg,i} = 15nm$ and $\sigma_i = 3nm$ where σ is the standard deviation and i denotes the axis (X, Y or Z). Each ellipsoid was rotated and its volume was adjusted to fit the volume of a single sphere with the radius $r_p = 15nm$. The

centres of primary particles did not change their positions, what resulted in some gaps and intersections. To adjust the volume of the investigated fractal-like aggregates and remove mentioned gaps, cylindrical connectors were implemented.[44–46] Cylinders were put between the centres of previously connected pairs of primary particles and their radii were $r_c \approx 4.8nm$ ($N_p = 25$), $r_c \approx 3.6nm$ ($N_p = 50$), $r_c \approx 3.6nm$ ($N_p = 75$) and $r_c \approx 2.7nm$ ($N_p = 100$) respectively. After this procedure the absolute relative volume error was lower than $|\delta V| < 0.05\%$ in every case. The volume correction procedure was not needed, and therefore, centres of primary particles remained exactly in the same position. One of the investigated geometries is presented in Fig. 11B. The light scattering results (see Fig. 12) were not averaged. Note, that when the absolute (not relative) extinction difference $\Delta C(\lambda)_{ext}$ is considered the diagrams are very similar to those presented in Fig. 6, regardless of the particle shape.

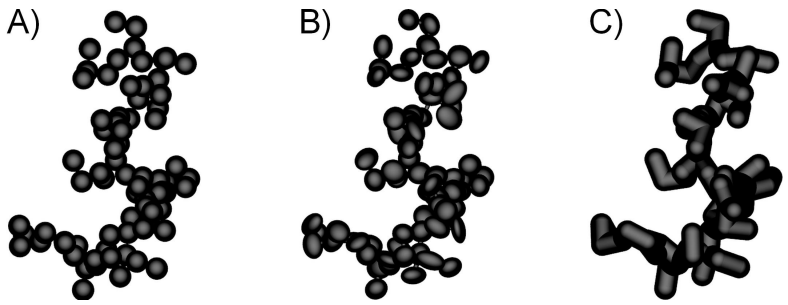

Figure 11. A) The initial fractal-like aggregate composed of $N_p = 75$ primary particles, B) Primary particles are non-spherical, C) Connections between primary particles are not negligible.

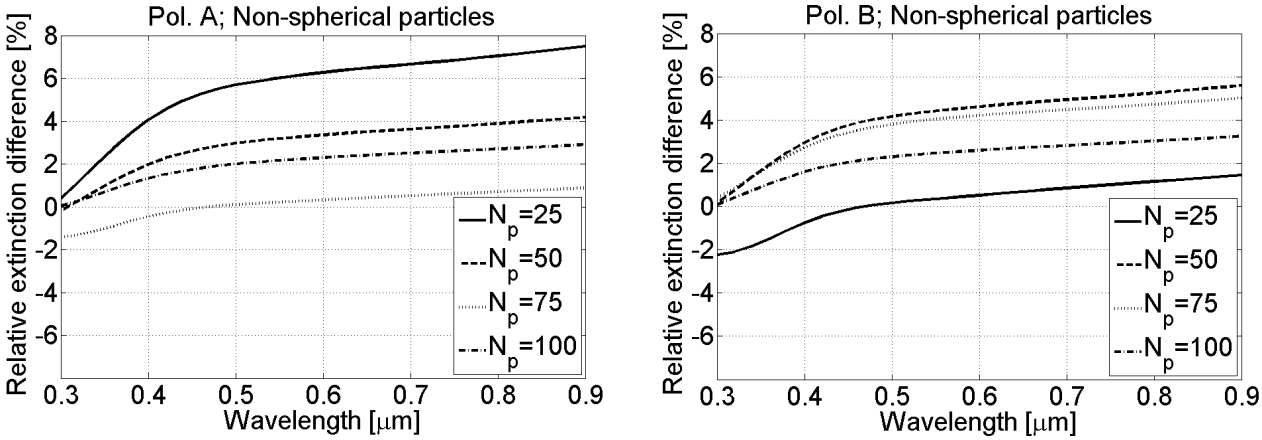

Figure 12. The relative extinction difference between aggregates composed of ellipsoidal particles and those made up of particles in point contact, see Fig. 6.

The influence of the necking phenomenon is presented in Fig. 13. As before, the volume correction procedure was not used and the light scattering results were not averaged. The radii of cylinders positioned between connected pairs of primary particles were $r_c = r_p = 15nm$ what resulted in increased volume of the scatterer (see Fig. 11C). The diagrams show that connections between primary particles alter the optical properties of investigated geometries, and therefore, large connections should not be neglected in fractal-like aggregate models.

Finally, the particle radius r_p was diminished to reduce the volume of the scatterer and make it more similar to the reference one, i.e. $\delta V < 0.05\%$. As before, the centres of primary particles remained in the same place. In this part of the study the particle radius was $r_p = r_c \approx 12.5nm$. The volume correction procedure was not used and results, which are presented in Fig. 14, were not averaged. They prove that thick necks should not be omitted in fractal-like aggregate models, even if the volume of the scatterer is conserved.

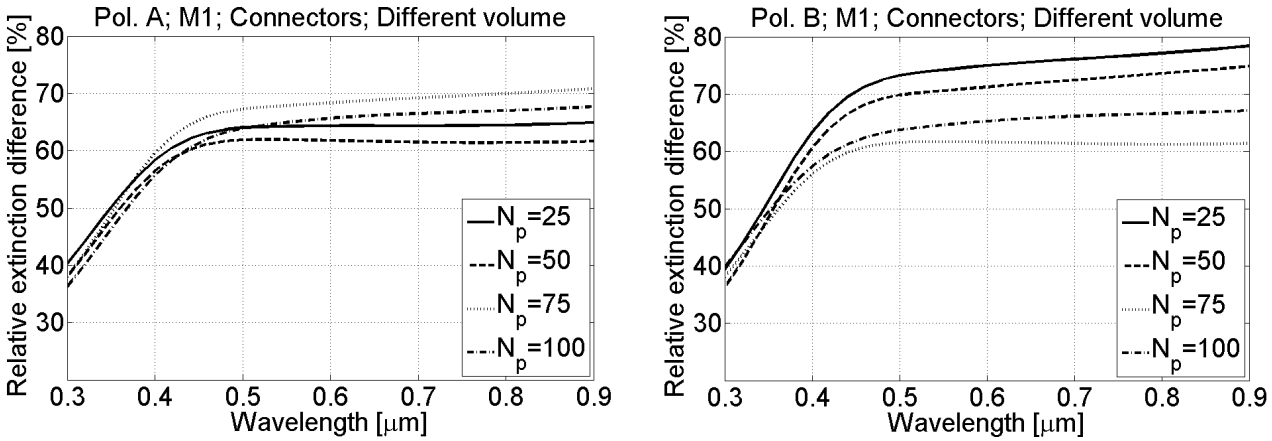

Figure 13. The relative extinction difference between aggregates enriched with cylindrical connectors and those made up of particles in point contact, see Fig. 6. The volume was not adjusted to fit the reference value.

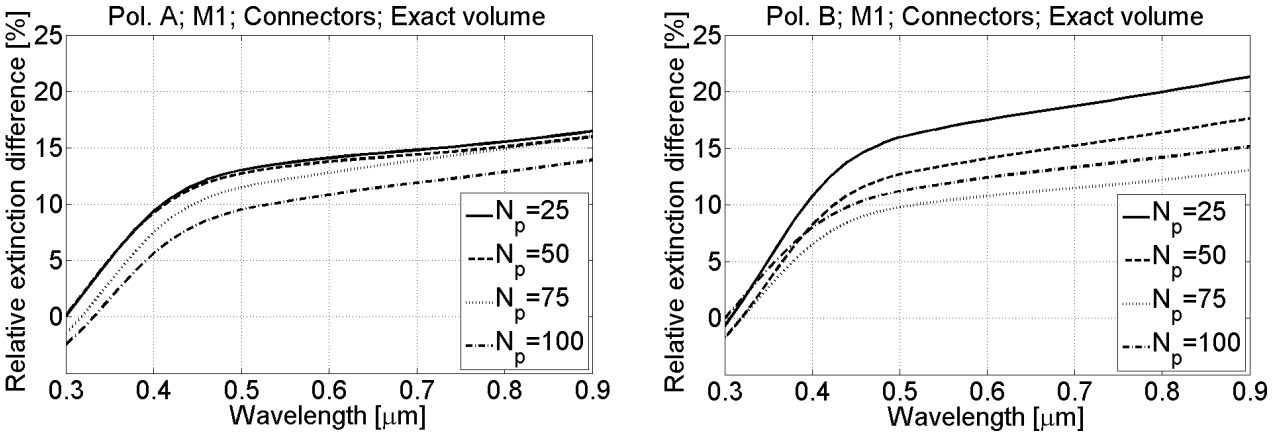

Figure 14. The relative extinction difference between aggregates enriched with cylindrical connectors and those made up of particles in point contact, see Fig. 6. The volume was adjusted to fit the reference value, i.e. the particle radius r_p was diminished.

3. CONCLUSIONS

The aim of this work was to investigate the impact of different BC geometries and simulation techniques on the extinction diagrams. The results might lead to more accurate fractal-like aggregate models that can be used in further study.[47] When a geometry is complex, e.g. when fractal-like aggregates are investigated, the volume correction procedure is not necessary. Furthermore, it can slightly shrink or enlarge the investigated geometry. Large connections between primary particles, due to their impact on the optical properties of BC aggregates, should always be taken into account, and therefore, included in fractal-like aggregate models. Non-spherical primary particles might alter extinction diagrams. These changes might be meaningful when very precise calculations are needed. Otherwise, primary particles can be modelled as spheres.

REFERENCES

[1] Sorensen, C. M., "Light scattering by fractal aggregates: A review," *Aerosol Science and Technology* **35**, 648–687 (2001).

[2] Riefler, N., Stasio, S., and Wriedt, T., "Structural analysis of clusters using configurational and orientational averaging in light scattering analysis," *Journal of Quantitative Spectroscopy and Radiative Transfer* **89**, 323–342 (2004).

[3] Skorupski, K., Mroczka, J., Riefler, N., Oltmann, H., Will, S., and Wriedt, T., "Impact of morphological parameters onto simulated light scattering patterns," *Journal of Quantitative Spectroscopy and Radiative Transfer* **119**, 53–66 (2013).

[4] Filippov, A., Zurita, M., and Rosner, D., "Fractal-like aggregates: Relation between morphology and physical properties," *Journal of Colloid and Interface Science* **229**, 261–273 (2000).

[5] Skorupski, K., Mroczka, J., Wriedt, T., and Riefler, N., "A fast and accurate implementation of tunable algorithms used for generation of fractal-like aggregate models," *Physica A: Statistical Mechanics and its Applications* **404**, 106–117 (2014).

[6] Meakin, P., "A historical introduction to computer models for fractal aggregates," *Journal of Sol-Gel Science and Technology* **15**, 97–117 (1999).

[7] Bond, T., "Spectral dependence of visible light absorption by carbonaceous particles emitted from coal combustion," *Geophysical Research Letters* **28**, 4075–4078 (2001).

[8] Bond, T., Doherty, S., Fahey, D., Forster, P., Berntsen, T., DeAngelo, B., Flanner, M., Ghan, S., Karcher, B., Koch, D., Kinne, S., Kondo, Y., Quinn, P., Sarofim, M., Schultz, M., Schulz, M., Venkataraman, C., Zhang, H., Zhang, S., Bellouin, N., Guttikunda, S., Hopke, P., Jacobson, M., Kaiser, J., Klimont, Z., Lohmann, U., Schwarz, J., Shindell, D., Storelvmo, T., Warren, S., and Zender, C. S., "Bounding the role of black carbon in the climate system: A scientific assessment," *Journal of Geophysical Research: Atmospheres* **118**, 5380–5552 (2013).

[9] Adachi, K., Chung, S., Friedrich, H., and Buseck, P. R., "Fractal parameters of individual soot particles determined using electron tomography: implications for optical properties," *Journal of geophysical research* **112**, D14202 (2007).

[10] Sorensen, C. M. and Feke, G. D., "The morphology of macroscopic soot," *Aerosol Science and Technology* **25**, 328–337 (1996).

[11] Poppel, L. L., Friedrich, H., Spinsby, J., Chung, S. H., Seinfeld, J. H., and Buseck, P. R., "Electron tomography of nanoparticle clusters: Implications for atmospheric lifetimes and radiative forcing of soot," *Geophysical Research Letters* **32**, L24811,doi:10.1029/2005GL024461 (2005).

[12] Chang, H. and Charalampopoulos, T., "Determination of the wavelength dependence of refractive indices of flame soot," *Proceedings: Mathematical and Physical Sciences* **430**, 577–591 (1990).

[13] Bond, T. and Bergstrom, R., "Light absorption by carbonaceous particles: an investigative review," *Aerosol Science and Technology* **40**, 27–67 (2006).

[14] Smyth, K. and Shaddix, C., "The elusive history of m=1.57-0.56i for the refractive index of soot," *Combustion and Flame* **107**, 314–320 (1996).

[15] Hess, M., Koepke, P., and Schult, I., "Optical properties of aerosols and clouds: The software package opac," *Bulletin of the American Meteorological Society* **79**, 831–844 (1998).

[16] Mroczka, J. and Szczuczynski, D., "Inverse problems formulated in terms of first-kind fredholm integral equations in indirect measurements," *Metrology and Measurement Systems* **16**, 333–357 (2009).

[17] Mroczka, J. and Szczuczynski, D., "Improved regularized solution of the inverse problem in turbidimetric measurements," *Applied Optics* **5**, 4591 (2010).

[18] Mroczka, J. and Szczuczynski, D. K., "Simulation research on improved regularized solution of the inverse problem in spectral extinction measurements," *Applied Optics* **51**, 1715–1723 (2012).

[19] Mroczka, J., Wozniak, M., and Onofri, F. R. A., "Algorithms and methods for analysis of the optical structure factor of fractal aggregates," *Metrology and Measurements Systems* **19**, 459–470 (2012).

[20] Will, S., Schraml, S., Bader, K., and A.Leipertz, "Performance characteristics of soot primary particle size measurements by time-resolved laser-induced incandescence," *Applied Optics* **37**, 5647–5658 (1998).

[21] Iuliis, S. D., Cignoli, F., and Zizak, G., "Two-color laser-induced incandescence (2C-LII) technique for absolute soot volume fraction measurements in flames," *Applied Optics* **44**, 7–8 (2005).

[22] Ryser, R., Gerber, T., and Dreier, T., "Soot particle sizing during high-pressure diesel spray combustion via time-resolved laser-induced incandescence," *Combustion and Flame* **156**, 120–129 (2009).

[23] Oltmann, H., Reimann, J., and Will, S., "Single-shot measurement of soot aggregate sizes by wide-angle light scattering (WALS)," *Applied Physics B: Lasers and Optics* **106**, 171–183 (2012).

[24] Oltmann, H., Reimann, J., and Will, S., "Wide-angle light scattering (WALS) for soot aggregates characterization," *Combustion and Flame* **157**, 516–522 (2010).

[25] Wozniak, M., Onofri, F. R. A., Barbosa, S., Yon, J., and Mroczka, J., "Comparison of methods to derive morphological parameters of multi-fractal samples of particle aggregates from tem images," *Journal of Aerosol Sciance* **47**, 12–26 (2012).

[26] Brasil, A. M., Farias, T. L., and Carvalho, G., "A recipe for image characterization of fractal-like aggregates," *Journal of Aerosol Science* **30**, 1379–1389 (1999).

[27] Czerwinski, M., Mroczka, J., Girasole, T., Gouesbet, G., and Grehan, G., "Light-transmittance predictions under multiple-light-scattering conditions. I. direct problem: hybrid-method approximation," *Applied Optics* **40**, 1514–1524 (2001).

[28] Czerwinski, M., Mroczka, J., Girasole, T., Gouesbet, G., and Grehan, G., "Light-transmittance predictions under multiple-light-scattering conditions. II. inverse problem: particle size determination," *Applied Optics* **40**, 1525–1531 (2001).

[29] Wriedt, T., "Light scattering theories and computer codes," *Journal of Quantitative Spectroscopy and Radiative Transfer* **110**, 833–8433 (2009).

[30] Purcell, E. M. and Pennypacker, C. R., "Scattering and absorption of light by nonspherical dielectric grains," *The Astrophysical Journal* **186**, 707–714 (1973).

[31] Draine, B. T. and Flatau, P. J., "Discrete dipole approximation for scattering calculations," *Journal of the Optical Society of America A* **11**, 1491–1499 (1994).

[32] Penttila, A., Zubko, E., Lumme, K., Muinonen, K., Yurkin, M., Draine, B., Rahola, J., Hoekstra, A., and Shkuratov, Y., "Comparison between discrete dipole implementations and exact techniques," *Journal of Quantitative Spectroscopy and Radiative Transfer* **106**, 417–436 (2007).

[33] Yurkin, M. and Hoekstra, A., "The discrete dipole approximation: An overview and recent developments," *Journal of Quantitative Spectroscopy and Radiative Transfer* **106**, 558–589 (2007).

[34] Yurkin, M. and Hoekstra, A., "The discrete-dipole-approximation code adda: Capabilities and known limitations," *Journal of Quantitative Spectroscopy and Radiative Transfer* **112**, 2234–2247 (2011).

[35] Yurkin, M., Min, M., and Hoekstra, A., "Application of the discrete dipole approximation to very large refractive indices: Filtered coupled dipoles revived," *Physical Review E* **82**, http://dx.doi.org/10.1103/PhysRevE.82.036703 (2010).

[36] Wriedt, T., Hellmers, J., Eremina, E., and Schuh, R., "Light scattering by single erythrocyte: Comparison of different methods," *Journal of Quantitative Spectroscopy and Radiative Transfer* **100**, 444–456 (2006).

[37] Nilsson, A., Alsholm, P., Karlsson, A., and Andersson-Engels, S., "T-matrix computations of light scattering by red blood cells," *Applied Optics* **37**, 2735–2748 (1998).

[38] Mroczka, J. and Wysoczanski, D., "Plane-wave and gaussian-beam scattering on an infinite cylinder," *Optical Engineering* **39**, 736–770 (2000).

[39] Girasole, T., Gouesbet, G., Grehan, G., Toulouzan, J. L., Mroczka, J., Ren, K., and Wysoczanski, D., "Cylindrical fibre orientation analysis by light scattering. part II: Experimental aspects," *Particle and Particle Systems Characterization* **14**, 211218 (1997).

[40] Girasole, T., Bultynck, H., Gouesbet, G., Grehan, G., Meur, F. L., Toulouzan, J. L., Mroczka, J., and Wysoczanski, D., "Cylindrical fibre orientation analysis by light scattering. part I: Numerical aspects," *Particle and Particle Systems Characterization* **14**, 163–174 (1997).

[41] Girasole, T., Toulouzan, J. L., Mroczka, J., and Wysoczanski, D., "Fiber orientation and concentration analysis by light scattering: Experimental setup and diagnosis," *Review of Scientific Instruments* **68**, 2805–2811 (1997).

[42] Skorupski, K., "Using the DDA (discrete dipole approximation) method in determining the extinction cross section of black carbon," *Metrology and Measurement Systems* **22**, 153–164 (2015).

[43] Mackowski, D. and Mischenko, M., "A multiple sphere t-matrix fortran code for use on parallel computer clusters," *Journal of Quantitative Spectroscopy and Radiative Transfer* **112**, 2182–2192 (2011).

[44] Skorupski, K. and Mroczka, J., "Effect of the necking phenomenon on the optical properties of soot particles," *Journal of Quantitative Spectroscopy and Radiative Transfer* **141**, 40–48 (2014).

[45] Skorupski, K., "Changes in the optical properties of two gold nanoparticles caused by different connection types," *SPIE 9126, Nanophotonics V, 912635* , doi:10.1117/12.2052319 (2014).
[46] Skorupski, K., Hellmers, J., Feng, W., Mroczka, J., Wriedt, T., and Mdler, L., "Influence of sintering necks on the spectral behaviour of ITO clusters using the discrete dipole approximation," *Journal of Quantitative Spectroscopy and Radiative Transfer* , doi:10.1016/j.jqsrt.2015.02.021 (2015).
[47] Mroczka, J., "The cognitive process in metrology," *Measurement* **46**, 2896–2907 (2013).